A Theoretical Model for Finite-Element Magnetoinductive Waveguides

Samuel Coogle, Connor Jenkins, and Asimina Kiourti
ElectroScience Laboratory, Dept. of Electrical and Computer Engineering, The Ohio State University, Columbus, OH 43212 USA (email: coogle.8@osu.edu)

***Abstract*—In this work, we present an alternative method for modeling finite-element magnetoinductive waveguides (MIWs) based on an equivalent circuit derivation. The proposed method provides practical insight into the behavior and operation of finite MIWs that cannot be fully explained using the dispersion model currently dominating MIW analysis, such as passband ripples. The model shows excellent agreement with simulated and experimental results when compared with first-order dispersion relation analysis and demonstrates the ability to predict behavior under complex MIW structures, such as junctions. To our knowledge, this is the first time that the equivalent circuit model presented in this work has been used to analyze MIW behavior and performance.**

Keywords— Circuit equivalent; electromagnetic modeling; magnetoinductive waveguide (MIW); magnetoinductive (MI) waves

I. Introduction

A magnetoinductive waveguide (MIW) is a structure formed from a closely-packed collection of electrically small, resonant loops that support the propagation of magnetoinductive (MI) waves. The dispersion relation defining MIW operation assumes an infinite MIW [1], i.e., there are no termination-induced reflections along the waveguide. When an MIW is restricted to finite length, the passband becomes uneven and rippled. Using the theory of an infinite MIW to approximate the operation of a real, finite-element MIW is typically reliable. However, in cases such as discontinuities, junctions, or severe impedance mismatch, the real passband of the MIW begins to deviate significantly from the predicted, theoretical passband.

In this work, we develop an equivalent circuit model for finite element MIWs. As a proof-of-concept, we use this model to predict the passband of an 11-loop axial MIW in three cases: (1) no loops are broken; (2) the loop closest to the transmitting (Tx) loop is broken; and (3) the middle loop (i.e., loop six) is broken. We then validate these predictions using both simulation and experimental results. These test-cases demonstrate the valuable insight on finite MIW behavior that can be quickly and accurately attained using this model. These cases also demonstrate the practical application of this model, as MIW loop breakage has only been studied previously via simulations for the application of Wireless Body Area Networks (WBANs) [2]. By developing a theoretical model with the ability to predict the passband behavior of finite length MIWs, we are empowering practical design considerations of real MIWs and MIW devices.

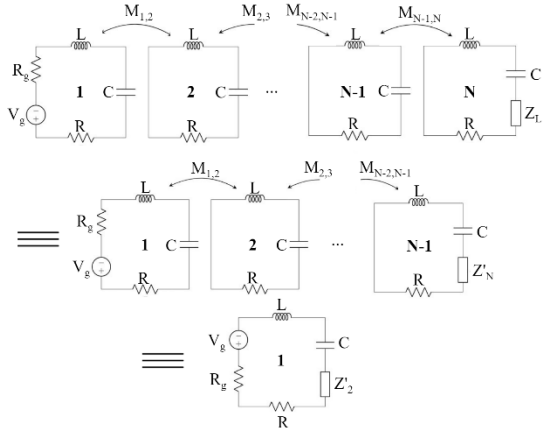

Fig. 1. Derivation of the equivalent circuit model used to analyze finite MIWs in this work.

II. Theoretical Model

A. Equivalent Circuit Model

We consider the general case of an N-element MIW shown at the top of Fig. 1. We assume the capacitance C, inductance L, and resistance R are the same for all loops to simplify our model. Further, we assume that coupling only occurs between directly neighboring loops. We do not require that the mutual coupling ($M_{x,y}$) between neighboring loops be uniform along the MIW.

We begin at loop N (i.e., the receive (Rx) loop) of the MIW and follow the iterative reduction process shown in Fig. 1. The impedance of the N^{th} loop is given by

$$Z_N = j(\omega L - 1/\omega C) + R + Z_L, \tag{1}$$

where Z_L is the terminal impedance, ω is the radial frequency and j is the complex unit. The circuit model, consisting of N loops, is reduced to N-1 loops by reflecting the impedance loop N onto loop N-l. The reflected impedance of loop N, Z'_N, is given by

$$Z'_N = \frac{\omega^2 M_{N-1,N}^2}{Z_N}. \tag{2}$$

Next, the impedance of loop N-1 (including the series impedance Z'_N) is reflected onto loop N-2. This process continues until the entire MIW is represented by one loop, as shown at the bottom of Fig. 1, where Z'_2 is the equivalent impedance of loops two through N as derived through this process. The real power dissipated by this impedance (R'_2) represents the power propagated beyond the first loop of the MIW.

We can now approximate the transmission coefficient of our MIW as

$$\tilde{S}_{21} = \frac{R_2'}{R_g + R + R_2'}. \quad (3)$$

This is an approximation as some of the power dissipated by R'_2 is the conduction loss as the MI wave propagates down the MIW. These conduction losses cannot be easily separated from the power dissipated by the termination due to the complex interaction between impedances as they are reflected.

B. Model Validation Setup

We consider an 11-loop MIW constructed of circular, axially aligned 4 cm radius loops. Each loop has the following parameters: R = 0.29 Ω, C = 470 pF, and L = 293 nH. The gap between neighboring elements is g = 2 cm. The MIW is terminated by an impedance Z_L = 50 Ω, and has a generator resistance of R_g = 50 Ω. Each loop is coupled to its direct neighbors with M = 19.8 nH. We construct a physical model (shown in Fig. 2(a)) and a simulation model (using CST Studio Suite [3]) for comparison to our theoretical results.

We consider this MIW under three different cases of mechanical failure: (1) no mechanical failure has occurred; (2) the middle loop (i.e., loop six) is broken; and (3) the second loop (from Tx) is broken. To perform our analysis in Cases 2 and 3, we remove the broken loop from the model. The direct neighbors of the broken loop are then coupled to each other with M' = 5.7 nH.

C. Results

Fig. 2(b), 2(c), and 2(d) show our results for Case 1, Case 2, and Case 3, respectively. Our model correctly predicts that Case 2 exhibits the lowest minimum path loss, and that Case 3 exhibits the highest minimum path loss. Our model also provides a qualitative estimate of the passband ripples and offers a good quantitative estimate for the path loss in each case; however, the theoretical results provided by our model are slightly shifted in frequency and exhibit a smaller bandwidth than the corresponding simulation results. Note that the circuit model can be extended to include non-nearest neighbor coupling which will lead to improved agreement.

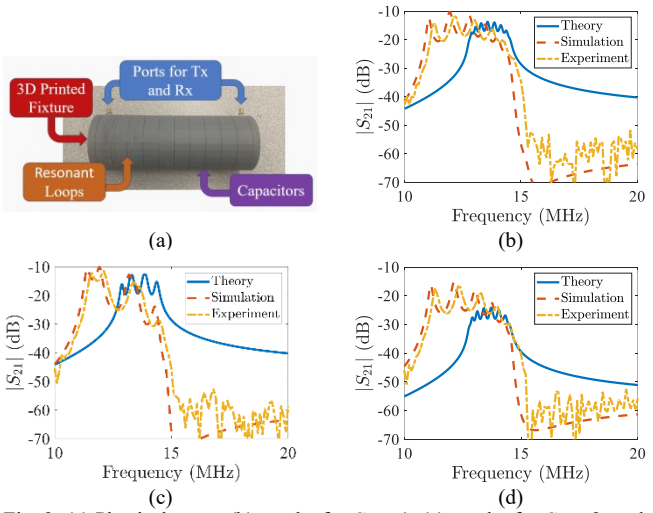

Fig. 2. (a) Physical setup, (b) results for Case 1, (c) results for Case 2, and (d) results for Case 3.

TABLE I
COMPARISON OF ANALYSIS TECHNIQUES

		This Work	Dispersion Relation	Experimental Results
Case 1	Min. Path Loss (dB)	-13.73	-7.46	-11.91
	Bandwidth (MHz)	2.0	1.7	3.2
Case 2	Min. Path Loss (dB)	-12.67	-13.24	-11.48
	Bandwidth (MHz)	1.9	1.7	2.6

D. Comparison to Dispersion Relation

We now analyze Cases 1 and 2 using the first-order dispersion relation and compare the results to our model. Case 2 is chosen as opposed to Case 3 due to simplicity of analysis under the dispersion relation. We assume no reflections at the termination (a necessary but poor assumption in the case of finite MIWs as broadband matching is challenging for these devices). We analyze Case 1 using the attenuation coefficient of this MIW. We analyze Case 2 by treating this structure as a mirror (described in [4]). The minimum path loss and 10-dB bandwidth are compared in Table I. In both cases, our model has stronger agreement with the experimental results than the predictions made using the dispersion relation.

III. CONCLUSION

We described a new model to analyze finite-element MIWs that can accurately predict phenomena occurring on finite MIWs (e.g., passband ripples) that are not described by previous analysis techniques. This model also accurately predicts changes in MIW performance due to irregularities such as junctions and discontinuities, problems that are very complex using previous models. We further demonstrated the capabilities of this model to accurately describe the behavior of a finite MIW in several test cases. Finally, we used a physical model to validate our results. Overall, the model developed in this paper provides an alternative method of analysis for finite MIWs that offers practical insight into the performance of real MIWs.

REFERENCES

[1] E. Shamonina, V. A. Kalinin, K. H. Ringhofer, and L. Solymar, "Magnetoinductive waves in one, two, and three dimensions," *Journal of Applied Physics*, vol. 92, no. 10, pp. 6252–6261, 2002. doi:10.1063/1.1510945

[2] V. Mishra and A. Kiourti, "Wearable Magnetoinductive Waveguide WBANs: Tolerance to Loop Failures," 2021 IEEE International Symposium on Antennas and Propagation and USNC-URSI Radio Science Meeting (APS/URSI), Singapore, Singapore, 2021, pp. 595-596, doi: 10.1109/APS/URSI47566.2021.9704216.

[3] *Electromagnetic Simulation Solvers CST Studio Suite*, Sep. 2022, [online] Available: https://www.3ds.com/products-services/simulia/products/cst-studio-suite/solvers/.

[4] R. R. A. Syms, E. Shamonina, and L. Solymar, "Magneto-inductive waveguide devices," *IEE Proceedings - Microwaves, Antennas and Propagation*, vol. 153, no. 2, pp. 111–121, Apr. 2006. doi:10.1049/ip-map:20050119